

Complex-Mode Buffeting Analysis of Long-Span Bridges

Nguyen Nguyen Minh*, Toshio Miyata** and Hitoshi Yamada***

* Graduate Student, Dept. of Civil Engineering, Yokohama National University

** Professor, Dept. of Civil Engineering, Yokohama National University

*** Assoc. Prof., Dept. of Civil Engineering, Yokohama National University

An analytical approach for buffeting response of long-span bridges using complex modes is presented. The approach can be performed in either frequency or time domain. The calculating scheme is based on the direct complex modal analysis of the three-dimensional model of long-span bridges in the presence of aeroelastic phenomena. By using complex modes, the actual modal characteristics integrating with aeroelastic effects can be effectively obtained at each mean wind speed. Coupled responses are therefore accurately captured. A numerical example is made for Akashi-Kaikyo Bridge. By the present method and using the turbulence generated in wind tunnel for the full-model experiment of the bridge as input, the calculated results agree very well with the experimental ones. Some effects by the uses of spatial coherence, turbulent spectra on the buffeting response are then addressed.

Key Words: buffeting response, complex mode, aeroelastic, spatial coherence

1. Introduction

The development of construction materials and technology has made the recent trend in the design of cable-supported bridges toward longer and lighter, which result in very flexible and very low-damped structural systems. Such bridges are therefore very susceptible to, and, as a consequence, exhibit very complicated responses under wind action. The most typical case is Akashi Kaikyo Bridge, which will be the longest bridge of the world with a main span of 1990m. The full-model of this bridge in wind tunnel exhibited a strongly coupled three-dimensional vibration under gusty wind. Prediction of such buffeting response therefore emerges as the major serviceability consideration in the design of long-span bridges.

Many methods for predicting buffeting response of long-span bridges have been proposed in both frequency and time domains. The most traditional one is the Admittance Single Mode method by Davenport (1962), which was exclusively based on quasi-static assumption for the formulation of aerodynamic forces. Simiu and Scalan¹⁰⁾ (1986) have further developed another Single Mode method in the presence of aeroelastic phenomena. Despite their simplicity, these methods are inapplicable for modern long-span bridges in the viewpoint of analyzing coupled responses. Recently, the rapid development of computer technology has urged many attempts to solve the problem in time domain by many approaches. Relative Velocity by Miyata, et al.⁷⁾ (1995) and Rational Functions by Boonyapinyo, et al.¹¹⁾ (1997) are typical among others. Jain, et al.³⁾ (1996) also proposed a Multi-Mode method in frequency domain. These methods permit to take into account the aerodynamic and structural couplings into the analysis. Coupled responses thus can be obtained.

However, almost all of these methods, as long as following the modal analysis approach, have based on the assumption that the modal characteristics do not vary with the change of wind speed. The mechanical eigenvectors (or mode shapes) of the system at zero wind speed condition thus have been widely used for the modal decomposition. This assumption, however, does not hold true for very long-span bridges. The measured buffeting responses of the full model test of Akashi Kaikyo Bridge have indicated a considerable evolution of the modal characteristics of the system due to the change of wind speed. This evolution has been successfully traced out by the Mode Tracing Method proposed by Dung, et al.¹⁾ (1996) for flutter prediction. In this study, an approach for buffeting analysis of long-span bridges via this method is presented. Direct complex modal analysis for 3-dimensional model of bridges is performed with the integration of aeroelastic effects. The actual modal dynamic behaviors at a certain wind speed can be accurately obtained and used for the modal decomposition. Coupled responses are therefore accurately analyzed. The method can be developed in both frequency and time domains.

Numerical example is made for Akashi-Kaikyo Bridge. There so far have been many analytical works attempting to predict the bridge's buffeting response. However, whereas the torsional and vertical responses were predicted fairly well, the horizontal response was greatly overestimated when compared to those of the experiment. By employing the present method and using the wind turbulence generated in wind tunnel for the bridge's full-model test as input, very good agreements between analytical and experimental results are obtained. The accuracy of the approach is therefore effectively proved. Effects of some characteristics of turbulence input to the response are clearly addressed.

2. Frequency Domain Formulation

2.1 Complex Modal Analysis

The equation of motion of a full-model bridge in the presence of aeroelastic phenomena can be expressed as,

$$\mathbf{M}\ddot{\mathbf{u}} + \mathbf{C}\dot{\mathbf{u}} + \mathbf{K}\mathbf{u} = \mathbf{F}_{ae} + \mathbf{F}_b \quad (1)$$

where \mathbf{M} , \mathbf{K} are mass and stiffness matrices formed by Finite Element method, \mathbf{u} is displacement vector, \mathbf{F}_{ae} is motion-dependent self-excited force depending on reduced frequency $K=\omega B/U$ (ω is circular frequency and U is mean wind speed), and \mathbf{F}_b is buffeting force. Other notations are depicted in Fig.1. Assume harmonic oscillation, \mathbf{F}_{ae} can be expressed as follows,

$$\mathbf{F}_{ae} = \begin{Bmatrix} L_{ae} \\ D_{ae} \\ M_{ae}/B \end{Bmatrix} = -\pi\rho B^2 \mathbf{F}_w \begin{Bmatrix} \ddot{y} \\ \ddot{z} \\ \ddot{\alpha} \end{Bmatrix} = -\pi\rho B^2 \mathbf{F}_w \ddot{\mathbf{u}} \quad (2)$$

where

$$\mathbf{F}_w = \begin{bmatrix} L_{yR} + iL_{yI} & L_{zR} + iL_{zI} & L_{\alpha R} + iL_{\alpha I} \\ D_{yR} + iD_{yI} & D_{zR} + iD_{zI} & D_{\alpha R} + iD_{\alpha I} \\ M_{yR} + iM_{yI} & M_{zR} + iM_{zI} & M_{\alpha R} + iM_{\alpha I} \end{bmatrix} \quad (3)$$

in which L_{ae} , D_{ae} , M_{ae} are aeroelastic lift, drag and moment respectively; ρ is air density; \mathbf{F}_w contains a full set of 9-complex unsteady coefficients (or equivalently 18 flutter derivatives), which exclusively depend on reduced frequency K . Integrate \mathbf{F}_{ae} to the left-hand side as an additional complex mass and neglect damping, Eq.(1) can be rewritten as

$$\mathbf{M}_F \ddot{\mathbf{u}} + \mathbf{K}\mathbf{u} = \mathbf{F}_b \quad (4)$$

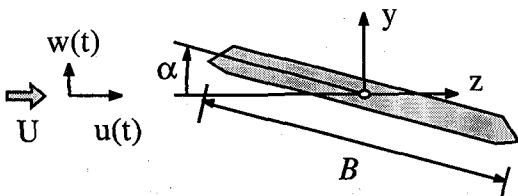


Fig.1: Sectional model of bridge deck

In \mathbf{M}_F , the self-excited force is integrated. Therefore \mathbf{M}_F is a complex function of reduced frequency K , whereas the buffeting force \mathbf{F}_b is a function of time. This contradiction make Eq.(4) impossible to be solved by a normal direct reduction to the modal space. Different frequencies of multi-mode system indicate that at a certain wind speed, each mode of structure has different reduced frequency. If following the technique of the Direct FEM Flutter Analysis⁸⁾, one can make the complex eigen-analysis for Eq.(4), which yields a set of modes with the same K , but at different mean wind speeds. This result is inapplicable in this case since the buffeting analysis needs a set of modes at a certain mean wind speed. In this sense, also based on this formulation, the Mode Tracing Method¹⁾ provides an

alternative. This method targets one mode at a time, and then step by step increases the mean wind speed to find the complex eigen-value by an iterative method. The eigen-values of many modes therefore can be determined and collected *at any prefixed wind speed*. The modal decomposition for Eq.(4) at a certain wind speed then can be performed by using corresponding eigenvectors. Since \mathbf{M}_F is complex and not symmetric, two biorthogonal sets of complex eigenvectors, left \mathbf{v}_L and right \mathbf{v}_R , exist for the modal decomposition. The left eigenvectors decide the contribution of external forces to each mode, whereas the rights express the mode shapes. The uncoupled equation of motion in generalized coordinate \mathbf{r} , where $\mathbf{u}=\mathbf{v}_R \mathbf{r}$, can be written as,

$$(\mathbf{v}_L^T \cdot \mathbf{M}_F \cdot \mathbf{v}_R) \ddot{\mathbf{r}} + (\mathbf{v}_L^T \cdot \mathbf{K} \cdot \mathbf{v}_R) \mathbf{r} = \mathbf{v}_L^T \cdot \mathbf{F}_b \quad (5)$$

However, this equation is in complex form, which makes it difficult to be solved. The more convenient and explicit form is,

$$\ddot{r}_i + 2\xi_i \omega_i \dot{r}_i + \omega_i^2 r_i = Q_{bi} \quad (6)$$

where $Q_{bi} = F_{bi} / m_i$; F_{bi} and m_i are modal buffeting force and modal mass. The modal aerodynamic damping ratio ξ_i and modal frequency ω_i here are real values as follows,

$$\omega_i = \sqrt{\lambda_{Ri}^2 + \lambda_{Ii}^2}; \quad \xi_i = \lambda_{Ii} / \sqrt{\lambda_{Ri}^2 + \lambda_{Ii}^2} + \xi_{si} \quad (7)$$

in which $\lambda_i = \lambda_{Ri} + i\lambda_{Ii}$ = square root of the corresponding complex eigenvalue, $i = \sqrt{-1}$; ξ_{si} is modal structural damping ratio. Taking the Fourier transform of Eq.(6) into the reduced frequency K domain, the equation of motion can be expressed as,

$$\mathbf{E}\bar{\mathbf{r}} = \bar{\mathbf{Q}}_b \quad (8)$$

where the overbar denotes the Fourier transform. Apparently, the impedance matrix \mathbf{E} here is completely diagonal. The general term is

$$E_{ii} = -K^2 + i(2\xi_i K_i)K + K_i^2 \quad (9)$$

in which, $K_i = \omega_i B / U$, and the aeroelastic effects determined by the unsteady coefficients (or flutter derivatives) has been integrated into mode shapes and other modal characteristics by direct complex eigen analysis via Mode Tracing method¹⁾. This is remarkably different from Multi-Mode approach³⁾, where \mathbf{E} has off-diagonal terms determined by flutter derivatives. Therefore, compared to other method, the modal characteristics of the present study are more refined since they are accurately determined at each mean wind speed. This is also the important advantage of the present method. Actual mode shapes and other modal properties at a mean wind speed are accurately known in prior, so that it is very easy to make judgments and select significant modes to include into the analysis. The coupled response also can be accurately captured and clearly explained by the complex mode shapes.

2.2 Buffeting Force

By quasi-steady assumption, the buffeting force F_b can be computed through a set of static coefficients from horizontal (u) and vertical (w) gust velocity components as follows

$$F_b = \begin{Bmatrix} L_b \\ D_b \\ M_b/B \end{Bmatrix} = \frac{\rho U B}{2} \begin{bmatrix} 2C_L (C'_L + C_D) \\ 2C_D & C'_D \\ 2C_M & C'_M \end{bmatrix} \begin{Bmatrix} u(t) \\ w(t) \end{Bmatrix} \quad (10)$$

where L_b , D_b , M_b are buffeting lift, drag and moment, respectively. C_L , C_D , C_M are static coefficients for lift, drag and moment, respectively. The prime (') denotes their derivatives with respect to the angle of attack of the mean wind speed on the section model (Fig.1). Values of these coefficients at the mean angle of attack α_0 are defined to be used.

The RMS of buffeting response can be obtained in term of power spectral density by solving Eq.(8) using standard random vibration analysis for MDOF system. A ready-developed form of this procedure convenient for bridge analysis can be found in the paper of Jain et al.³⁾ (1996). In this study, Eqs.(11) to (18) are employed from this procedure with an important revision that the left and right eigenvectors are appropriately used in each stage for consistency with the complex modal analysis. The general term of the power spectral density (PSD) matrix of buffeting force can be written as,

$$S_{Q_{bi}Q_{bj}}^* = \left(\frac{\rho B^3}{2U} \right)^2 \frac{1}{m_i m_j} \int_0^L \int_0^L \Psi(x_A, x_B, K) dx_A dx_B \quad (11)$$

where

$$\begin{aligned} \Psi(x_A, x_B, K) = & \left\{ \tilde{q}_i(x_A) \tilde{q}_j(x_B) S_{uu}(x_A, x_B, K) \right. \\ & + \tilde{s}_i(x_A) \tilde{s}_j(x_B) S_{ww}(x_A, x_B, K) \\ & + \left[\tilde{q}_i(x_A) \tilde{s}_j(x_B) + \tilde{s}_i(x_A) \tilde{q}_j(x_B) \right] C_{uw}(x_A, x_B, K) \\ & \left. + i \left[\tilde{q}_i(x_A) \tilde{s}_j(x_B) - \tilde{s}_i(x_A) \tilde{q}_j(x_B) \right] Q_{uw}(x_A, x_B, K) \right\} \quad (12) \end{aligned}$$

L is bridge's length; x_A , x_B are span locations; S_{uu} , S_{ww} , S_{uw} are respectively uu -cross-spectrum, ww -cross-spectrum and uw -cross-spectrum between 2 points x_A and x_B ; $S_{uw} = C_{uw} + iQ_{uw}$; with C_{uw} being cospectrum and Q_{uw} being quadrature spectrum; and

$$\tilde{q}_i(x) = 2[C_L y_{Li}(x) + C_D z_{Li}(x) + C_M \alpha_{Li}(x)] \quad (13)$$

$$\tilde{s}_j(x) = (C'_L + C_D) y_{Lj}(x) + C'_D z_{Lj}(x) + C'_M \alpha_{Lj}(x) \quad (14)$$

in which $y_{Li}(x)$, $z_{Li}(x)$ and $\alpha_{Li}(x)$ are respectively the vertical, horizontal and torsional components of the corresponding *left eigenvector* at span location x ; C_L , C_D , C_M are static coefficients for lift, drag and moment respectively. The prime (') denotes their derivatives with respect to the angle of attack. The PSD matrix for the generalized coordinate r is,

$$S_{rr}(K) = E^{-1} S_{Q_b Q_b} [E^*]^{-1} \quad (15)$$

Then, the PSD for physical displacements at x are

$$S_{yy}(x, K) = \sum_i \sum_j y_{Ri}(x) y_{Rj}(x) S_{r_i r_j}(K) \quad (16)$$

$$S_{zz}(x, K) = \sum_i \sum_j z_{Ri}(x) z_{Rj}(x) S_{r_i r_j}(K) \quad (17)$$

$$S_{\alpha\alpha}(x, K) = \sum_i \sum_j B^{-2} \alpha_{Ri}(x) \alpha_{Rj}(x) S_{r_i r_j}(K) \quad (18)$$

where i and j are number of modes. $y_{Ri}(x)$, $z_{Ri}(x)$ and $\alpha_{Ri}(x)$ are respectively the vertical, horizontal and torsional components of the corresponding *right eigenvector* at span location x . The mean-square values of buffeting response then can be evaluated by taking the integration of the respective physical displacement PSD with respect to frequency $f = KU/2\pi B$ from 0 to ∞ .

According to the theory of extreme statistics¹⁰⁾, the expected values of the maximum vibrational response occurring in the time interval T is

$$P_{max}(x) = k_p(x) \sigma_p(x) \quad (19)$$

where p stands for y , z or α displacement component; σ_p is the root-mean-square of p -component response; k_p is the respective peak factor, which can be estimated as

$$k_p(x) = [2 \ln v(x) T]^{1/2} + \frac{0.577}{[2 \ln v(x) T]^{1/2}} \quad (20)$$

in which

$$v(x) = \left[\frac{\int_0^\infty f^2 S_{pp}(x, f) df}{\int_0^\infty S_{pp}(x, f) df} \right]^{1/2} \quad (21)$$

$S_{pp}(x, f)$ is calculated from Eqs (16), (17), (18) with K replaced by real frequency f . Although S_{pp} is mostly narrow-banded, the estimation of the zero-upcrossing frequency $v(x)$ by using S_{pp} as a 'weighted function' as in Eq(21) is necessary due to the existence of multi-mode and coupled responses.

In the above buffeting force formulation, there are two assumptions. First, the so-called aerodynamic admittance functions are assumed to be 1. These frequency dependent functions account for the imperfect correlation of wind pressure around the deck's section, and would approach unit at low frequency range as suggested by Davenport's and Sears' functions⁷⁾. Second, the spatial coherence functions of respective components of buffeting forces along the bridge deck are assumed to be identical to those of the undisturbed turbulence velocity components of wind field. These assumptions are justifiable due to the fact that frequencies of the significant modes of a very long-span bridge are usually very small. Evidence for this fact can be seen for Akashi-Kaikyo Bridge later. Anyway, the present approach is ready for incorporating these aspects if the information is available.

In Eq.(10), the steady part of buffeting force due to mean wind speed is excluded, and therefore only dynamic response due to fluctuating part (zero mean) are the values of interest. This is a fair simplification. The present method is for linear system. Excluding the mean wind-induced response, the dynamic response is small enough for the linear analysis scheme to be valid. On the contrary, the static displacements due to the steady force of a long-span bridge are known to be very large⁶⁾. For this, a non-linear analysis scheme would be needed to include the geometric nonlinearity of structures. This non-linear effects may considerably alter the stiffness of structure at the static-displacement position, and hence inversely affect the buffeting and flutter response as well. A treatment for this problem was reported in Dung et al.²⁾.

3. Time-Domain Formulation

The formulation in time domain is similar to that in frequency domain until Eq.(7). The buffeting force is calculated directly from the time-histories of gust velocity components $u(t)$ and $w(t)$ by quasi-steady assumption in Eq.(10). The buffeting analysis is then carried out by direct integration method for Eq.(6). Time-histories of displacement responses, including vertical, horizontal and torsional components, can be obtained at any nodal point on the bridge deck. The RMS and ensemble average of maximum amplitude of the responses then can be evaluated from the time-histories.

The context of the approach thus involves the work of numerical simulation of wind turbulence $u(t)$ and $w(t)$. Details of this work can be found in Minh et al.⁵⁾. For the context, hereafter are some brief descriptions.

The numerical simulation of wind turbulence is made by Auto Regressive-Moving Average (ARMA) method. The generating algorithm of this method developed by Samaras et al.⁹⁾ for a multi-variate random stationary process is used. The two velocity components of wind turbulence, along-wind (u) and vertical (w), are generated simultaneously and spatially, so that the spatial correlation between these components can be fully taken into account.

The target input of the simulation is the spatial correlation function matrix. The elements of this matrix are created by inverse Fourier transform of the respective cross-spectra, which is estimated from the knowledge of the auto-spectra, point cross-spectrum and spatial coherence functions of wind turbulence.

Various checks on the simulated results show that the simulation can be effectively performed at very small values of time step with very good accuracy. The validity of the simulation is therefore improved and reliable for an analysis in time domain.

4. Numerical Example - Akashi-Kaikyo Bridge

Akashi-Kaikyo bridge, which will be the longest bridge in the world after completed in 1998, consists of a main span of 1990 m and two side spans of 960 m each. Buffeting response of the bridge has been obtained experimentally by a full model test in wind tunnel⁶⁾. In this study, the buffeting analysis for the bridge is

performed by the presented approach in both frequency and time domains. However, the results by frequency domain will be mainly presented. The results by time domain will be used for a comparison.

4.1 Turbulence characteristics

As previously presented, both calculated schemes in frequency or time domain need auto-spectra, point cospectrum, point quadrature-spectrum and spatial coherence functions of the turbulence velocity components as input. The spatial cross-spectrum is then evaluated by simply multiplying the auto-spectra (or point cospectrum) with the corresponding square-root of coherence functions. The quadrature spectrum is neglected in this study because its information is not available, and it appears to be very small however.

Since the buffeting response of the full model of Akashi-Kaikyo Bridge was obtained under the action of the turbulent flow generated in wind tunnel, the analytical results may better agree with the experimental results if the wind-tunnel turbulence characteristics are used as input. To check this idea, a comparative analysis is made here. Two cases of turbulence, named (a) and (b), are used for the buffeting calculation of the bridge. Case (a) is the turbulence with characteristics proposed from literature (hereafter called 'literature turbulence'), and case (b) is the turbulence generated in wind tunnel for the full-model test (hereafter called 'wind-tunnel turbulence').

(a) Characteristics of Literature Turbulence

After Kaimal et al.⁴⁾, the Auto-spectra S_u , S_w , and the Cospectrum Co_{uw} of natural turbulence can be expressed as,

$$\frac{f S_u(f)}{u^*{}^2} = \frac{105 f_r}{(1 + 33 f_r)^{5/3}} ; \quad \frac{f S_w(f)}{u^*{}^2} = \frac{2 f_r}{1 + 5.3 f_r^{5/3}} ;$$

$$\frac{f Co_{uw}(f)}{u^*{}^2} = \frac{-14 f_r}{(1 + 9.6 f_r)^{2.4}} \quad (22)$$

where f is frequency, f_r is reduced frequency, u^* is friction velocity. The conventional coherence function of the same velocity component at two points $P_1(x_1, y_1)$ and $P_2(x_2, y_2)$ is given by Davenport¹⁰⁾,

$$\sqrt{Coh(f)} = e^{-\hat{f}}$$

$$\text{where } \hat{f} = \frac{f \sqrt{C_x^2(x_1 - x_2)^2 + C_y^2(y_1 - y_2)^2}}{0.5(U_{y1} + U_{y2})} \quad (23)$$

in which, $C_x = 10$; $C_y = 16$

For the coherence function of u and w at different points, there is no information in literature.

(b) Characteristics of Wind Tunnel Turbulence

The time-history records of the horizontal velocity $u(t)$ and vertical velocity $w(t)$ of the wind-tunnel turbulence at 6 points along the bridge deck of the full-model test are analyzed to extract its statistical

characteristics. After scaled by the similarity rule, the scaled spectra and point cospectrum of the turbulence can be expressed as,

$$\frac{S_u(f)}{u^2} = \frac{8.7}{(1+12f)^{5/3}}, \quad \frac{S_w(f)}{u^2} = \frac{1.11}{1+8.97f^{5/3}}$$

$$\frac{Co_{uw}(f)}{u^2} = \frac{-2.56}{(1+5f)^{2.4}} \quad (24)$$

where $\overline{u^2}$ is mean square of gust component u . The coherence functions can be expressed in our proposed forms as follows,

$$Coh_{u_A u_B}(f) = C_0^u(dx) \exp(-f C_x^u dx / U) \quad (25)$$

$$Coh_{w_A w_B}(f) = C_0^w(dx) \exp(-f C_x^w dx / U) \quad (26)$$

$$Coh_{u_A w_B}(f) = 0.5 [Coh_{u_A u_B}(f) + Coh_{w_A w_B}(f)] \quad (27)$$

where $C_x^u = 12$, $C_x^w = 8$;

$$C_0^u(dx) = (1 - 0.001dx - 0.0003dx^2)$$

$$C_0^w(dx) = (1 - 0.03dx + 0.0002dx^2) \quad (28)$$

4.2 Buffeting Responses and Discussions

The finite element 3-D frame model of the bridge (Fig.2) is used for the numerical example of the present method. The buffeting response is calculated at six levels of mean wind speed: $U=30, 40, 50, 60, 70, 80$ m/s. Turbulence intensity $I_u=9.6\%$, $I_w=6\%$. The sets of flutter derivatives and static coefficients of the bridge at zero angle of attack¹²⁾ are used. Modal structural damping logarithmic decrements are approximately 0.03. Number of modes to be used is 32. This is a primary choice to include the 3rd modes of all components for a preliminary conservative analysis. The results of the investigation will show later that only very few modes actually involve in the response.

For the analysis in frequency domain, the frequency step to be used is $\Delta f=0.001$ Hz, which is fine enough to well tuned to the modal frequencies to obtain good results. For the analysis in time domain, the time step for the turbulence simulation and the Newmark β direct integration is 0.1 second. Duration to obtain response is 150 minutes. This duration is equivalent to the 15-minute response of the full model test, for which the experimental results are available for comparison.

(a) Comparative check of turbulence input

Results of the comparative analysis between Case (a) 'Literature turbulence' and Case (b) 'Wind-tunnel turbulence' are shown in Fig.3. The analytical torsional and vertical RMS responses agree very well with the experimental results in both cases of turbulence. The horizontal RMS response, which is highly overestimated for case (a), is greatly smaller and thus very well agrees with experimental result in case (b). Similar results are also obtained for the maximum vibrational amplitude.

A closer look into the dynamic behaviors of the bridge reveals that the horizontal response is governed

mainly by the 1st symmetric horizontal mode, which has a very low frequency of around 0.038 Hz. At this frequency, the Davenport's coherence function gives very high coherence of $u(t)$ along the bridge deck, but the wind-tunnel turbulence has much smaller values of the coherence for a well-separate distance as $dx=50$ m in Fig.5. Sensitive checks point out that this is the main cause of the overestimation for horizontal response when using literature turbulence as input. Moreover, higher values of S_u spectrum of literature turbulence than those of wind-tunnel turbulence at low-frequency range as seen in Fig.6 contribute some more errors to a smaller extent. These interesting results prove the correctness of the idea of using the wind-tunnel turbulence as input for a better match with the condition in wind tunnel, and also effectively prove the accuracy of the present approach.

(b) Comparison of frequency and time domain

Fig. 4 shows the comparison of RMS and maximum vibrational amplitude between the experimental and analytical results in both frequency and time domains. Very good agreements between them for all three displacement components confirm the stability of the formulation. An extra conclusion from this comparison is that the simulated turbulence⁵⁾ has good validity and is reliable for dynamic analysis in time domain.

Concerning the computational efforts, the frequency domain approach is very sensitive to the number of modes to be used. When the number of modes increases in linear order, the time consumption for the frequency domain increases almost in quadratic order due to the cross-modal calculation by matrix multiplication. On the contrary, the direct integration for the time domain very quickly solves the problem with the time consumption also linearly increasing. The time domain spends most of its computational time for generating the turbulent velocity components at a number of nodal points to apply the buffeting forces. However, which approach would be more computational efficient is not conclusive here since there are many other factors to consider for such a comparison. Anyway, for information, with the input data described in this numerical example, the frequency domain is twice faster than the time domain to solve Eq.(6). For a level of wind speed, time consumption of the frequency and time domains are respectively around 13 and 25 minutes on a Hewlett Packard Workstation HP 9000/700. Note that the time for modal decomposition, which is the same for both domains, is not included.

However, concerning the contains of the results, the results from the time domain are more informative than those of the frequency domain. The time domain results give the time-histories of responses, which are useful for the representation of instant response at any time, and for graphically visualized simulation of the response. These practices have emerged to be important and necessary for better understanding the dynamic behaviors of such a long-span bridge.

(c) Representation of coupled responses

A more detailed dynamic behaviors of the bridge can be observed by Figs.7 and 8, in which the evidences of coupled motions in the response can be seen clearly.

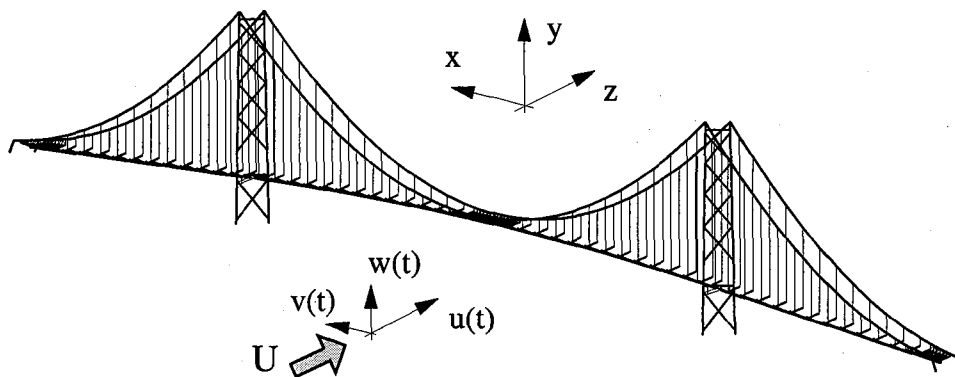


Fig.2: Three-dimensional model of Akashi Kaikyo Bridge in wind field

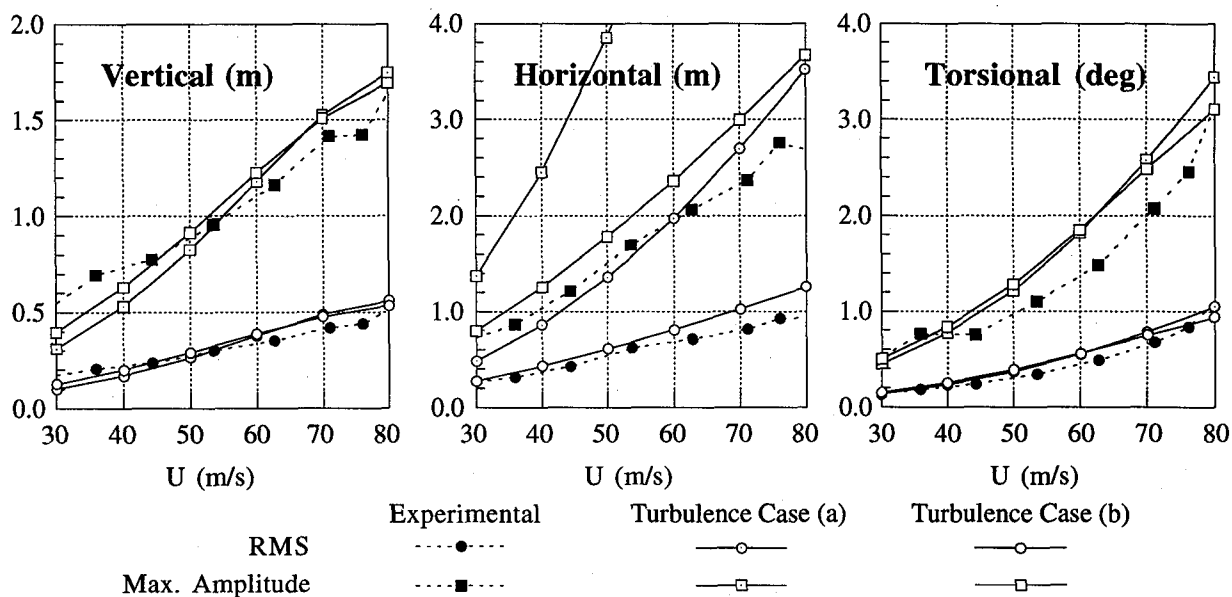


Fig. 3: Comparative check for different cases of turbulence input (by frequency domain)

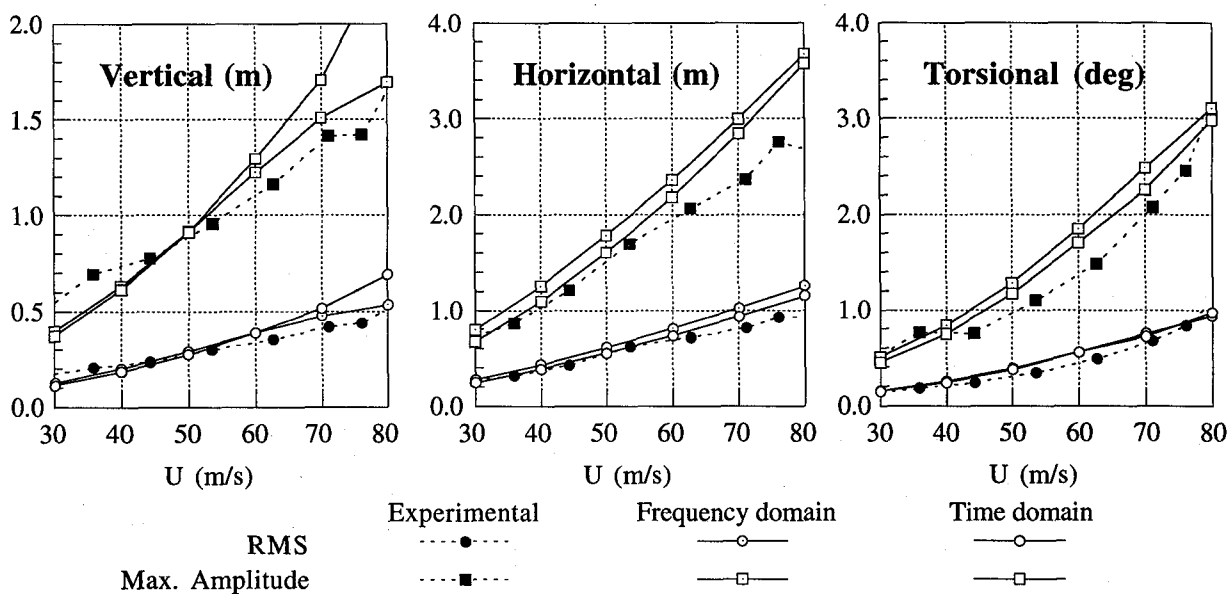


Fig. 4: Comparison of experimental and analytical results in frequency and time domain

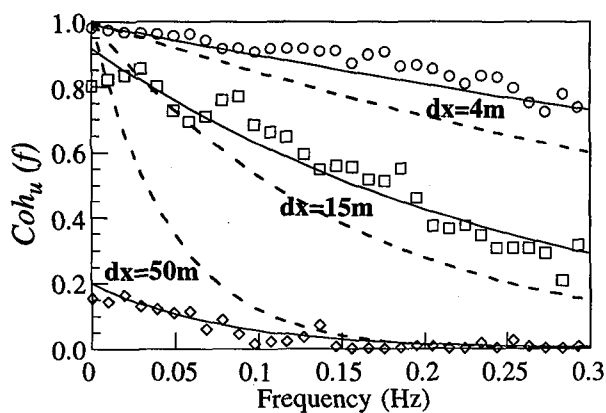


Fig. 5: Comparison of u -coherence functions
Symbol & line: wind tunnel's & fitted by Eq.(25)
Dash line: Davenport's

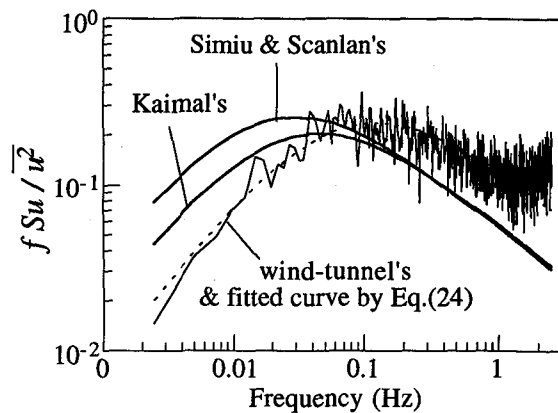


Fig. 6: Comparison of Auto-spectrum S_u

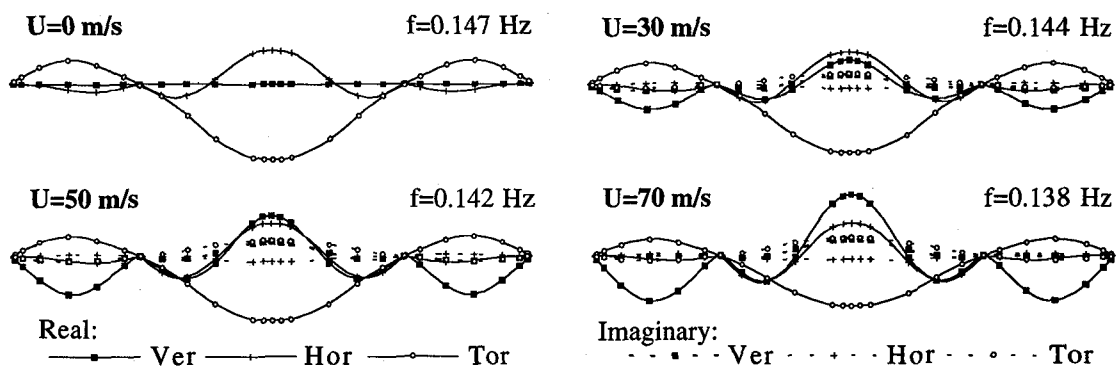


Fig. 7: Evolution of mode shape and modal frequency of coupled mode #10

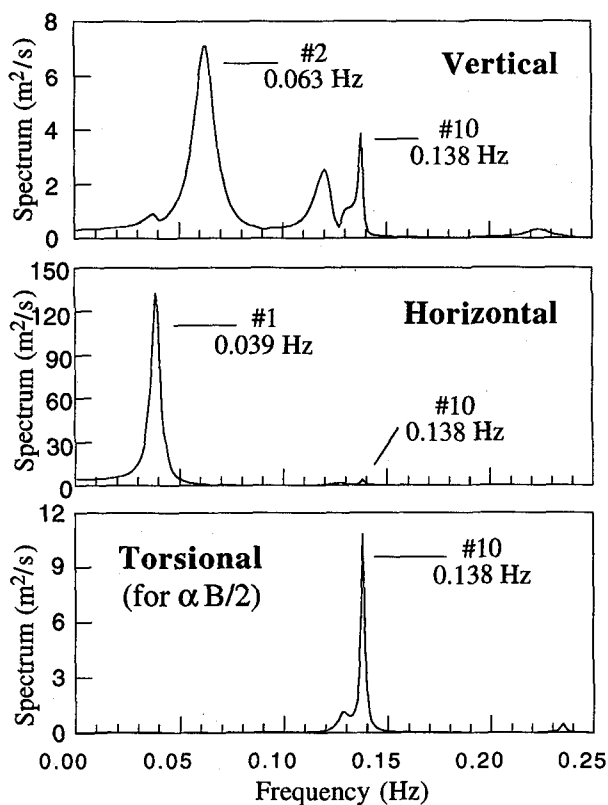


Fig. 8: Response Spectra at mid-span at $U=70$ m/s

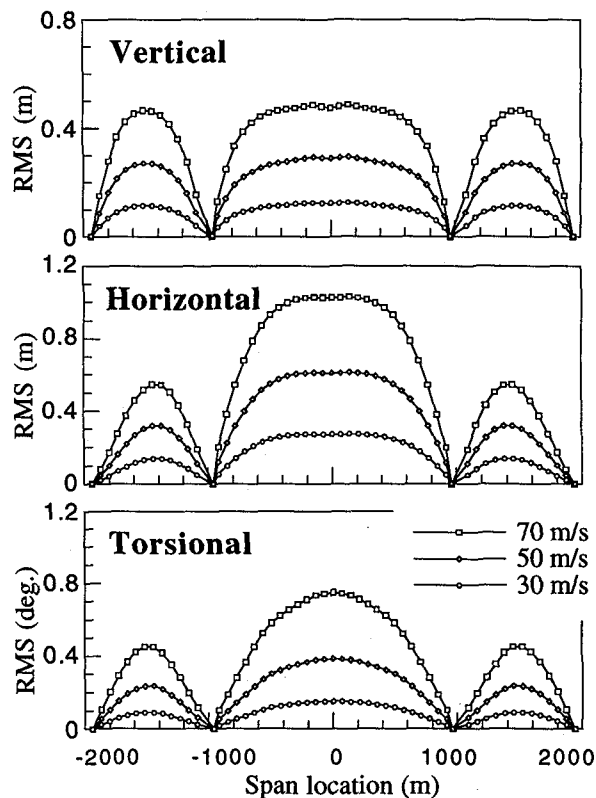


Fig. 9: RMS along the bridge's deck

Fig.7 shows the evolution of mode #10 at $U=0, 30, 50$ and 70 m/s. As the mean wind speed increases, notable coming into existence and development of the vertical component in the complex mode shape are observed, making the response more and more 3-dimensionally coupling at this modal frequency. This coupled motions obviously does not exist in the mechanical mode shape (at $U=0$). The modal frequency also gradually decreases from $f=0.147\text{Hz}$ to $f=0.138\text{Hz}$. The mode shape at high wind speeds thus exhibits strongly aeroelastic couplings between all three vibrational components. Another visualized evidence of the coupled response at high wind speeds can be seen by the response spectra of the middle of the main span at $U=70$ m/s as shown in Fig.8. Though each displacement component is mainly dominated by its own significant mode, all of them also have peaks of almost the same order of magnitude at mode #10 ($f=0.138$ Hz) (note that the peak of horizontal component appears small in the figure due to vertical scaling). Therefore, at high wind speeds, the buffeting response exhibits strongly 3-dimensional aeroelastic coupled motion at this frequency, which can be effectively analyzed by using complex mode shapes. The structural couplings between modes in the response are also clearly obtained. This mode #10 actually develops to flutter instability at higher wind speeds.

(d) Some other results and checks

From Fig.8, it can be seen that the estimation of the zero-upcrossing frequency $\nu(x)$ by Eq. (21) is necessary, especially for vertical displacement due to the multi-mode contribution. However, for the other components, the modal frequency of mode #1 (for horizontal) and mode #10 (for torsional) can be used instead.

Fig.9 shows the RMSs of response along the bridge's deck at $U=30, 50, 70$ m/s. The shape of these along-deck RMSs at $U=70$ m/s reflects very well the dynamic behavior of the bridge at this wind speed, where mode #10 becomes the dominant mode of the total response.

A check on significant modes indicates that the responses at the midspan of the main span are mainly contributed by only 5 modes: #1 (1st horizontal), #2 (1st vertical), #8 (3rd vertical), #9 and #10 (3-component coupling modes of 1st torsional, 3rd vertical and 3rd horizontal). The results by these modes are less-than-2% smaller than the results by 32 modes. Note that the frequencies of these modes are all very low at less than 0.15 Hz, so that the assumptions for buffeting forces' formulation can be justifiable.

The effects of the uw -correlation on the buffeting response have been a question in literature. In this study, the effects of this correlation on the response at the midspan are checked. When the correlation is excluded, the vertical response is overestimated around 10%, the torsional response is underestimated around 7%, and the horizontal response negligibly changes, compared with the results when the correlation is included. These results are in accordance with the negativeness of the correlation and the coupled behaviors of the response.

5. Conclusions

The presented buffeting calculation scheme has been proved to be very effective and practical. Since the

modal characteristics are accurately obtained at each mean wind speed, the aeroelastic effects can be comprehensively incorporated. The process of modal decomposition then becomes very straight forward. This makes the present method easy to develop in both frequency and time domains. By using complex mode shapes, coupled responses are accurately captured and clearly interpreted. The numerical example for Akashi-Kaikyo bridge results in some interesting findings, from which the roles of the turbulence input, especially the spatial coherence functions can be pointed out. The presented buffeting schemes here together with the Mode Tracing method¹⁾ for flutter analysis indeed effectively provide a consistent treatment for aerodynamic problem of long-span bridges, expectedly even in case of a longer span being encountered.

References

1. Dung, N.N., Miyata, T. and Yamada, H. (1996). "The Mode Tracing Method for Flutter of Long Span Bridges", *Proc., 14th Nat. Symposium on Wind Engrg.*, Kyoto, Japan, 1996.
2. Dung, N.N., Miyata, T. and Yamada, H. and Minh, N.N. (1997), "Flutter Responses in Long Span Bridges with Wind Induced Displacement by the Mode Tracing Method", *Proc., 8th Nat. US Conf. of Wind Engrg.*, Baltimore, USA, 1997.
3. Jain, A., Jones, N. P., and Scanlan, R. H. (1996). "Coupled Flutter and Buffeting Analysis of Long-Span Bridges," *J. Struct. Engrg.*, ASCE, 122(7).
4. Kaimal, J.C. et al. (1972), "Spectral Characteristics of Surface-Layer Turbulence", *Quart. Journal of Royal Meteorology Society*, Vol. 98.
5. Minh, N. N., Miyata, T., and Yamada, H. (1997). "Numerical Simulation of Wind Turbulence and Buffeting Analysis of Long Span Bridges," *Proc., 4th Asia-Pacific Symposium on Wind Engrg.*, Gold Coast, Australia, 1997.
6. Miyata, T. et al. (1995), "Full-Model Wind Tunnel Study on the Akashi Kaikyo Bridge," *Proc., 9th Int. Conf. on Wind Engrg.*, New Delhi, India, 1995.
7. Miyata, T. et al. (1995), "Analytical Investigation on the Response of a Very Long Suspension Bridge under Gustly Wind," *Proc., 9th Int. Conf. on Wind Engrg.*, New Delhi, India, 1995.
8. Miyata, T. and Yamada, H. (1988), "Coupled Flutter Estimate of a Suspension Bridge", *J. of Wind Engrg.*, 37, Japan.
9. Samaras, E. et al. (1985), "ARMA Representation of Random Processes", *J. Engrg. Mech.*, ASCE, 111.
10. Simiu, E. and Scanlan, R.H. (1986), *Wind Effect on Structures*, 2nd Ed., John Wiley and Sons, Newyork.
11. Virote Boonyapinyo, Miyata, T., and Yamada, H. (1997). "Combined Flutter and Buffeting Response of Suspension Bridges in Time Domain," *Proc., 4th Asia-Pacific Symp. on Wind Engrg.*, Australia.
12. Sudou S. (1997), "Comparative Study on Response of a Long Span Bridge in New Concepts of Unsteady Aerodynamic Force and Aeroelastic Response Analysis", *Master Thesis*, Dept. of Civil Engrg., Yokohama National University, Japan.

(Received on September 26, 1997)